

S/D Contact Solutions to Enable Contact Resistivity <1E-9 for 5nm and Beyond

Chih-Yang Chang, Fareen Adeni Khaja, Kelly E Hollar, KV Rao, Samuel Munnangi, Yongmei Chen, Motoya Okazaki, Yi-Chiau Huang, Xuebin Li, Hua Chung, Osbert Chan, Christopher Lazik, Miao Jin, Hongwen Zhou, Abhilash Mayur, Raymond Hung, Namsung Kim

Applied Materials 3050 Bowers Avenue, Santa Clara, CA 95053, USA

Phone: +1-408-584-0582 E-mail: chih-yang_chang@amat.com

ABSTRACT

In this paper, we present solutions for N&P MOS contact resistivity (ρ_c) improvement by adoption of highly doped epitaxial source/drain (S/D), contact ion implantation and advanced laser anneal. An ultra-low $\rho_c = 9.01 \times 10^{-10} \Omega\text{cm}^2$ on NMOS contact chain (CC) is achieved using highly doped (HD) Si:P selective epi in S/D combined with Ge PAI (pre-amorphization implant) and Applied Materials' nanosecond laser anneal (NLA). In addition, a record low $\rho_c = 1.16 \times 10^{-9} \Omega\text{cm}^2$ for PMOS CC is demonstrated by $\text{Si}_{0.55}\text{Ge}_{0.45}\text{:B}$ epi, Ga cryo ion implant and NLA. NLA enables super-activation of implanted dopants and dopants in the *in-situ* HD S/D epi films ([P]: $3.0 \times 10^{21}\text{cm}^{-3}$ for NSD epi; [B]: $1.0 \times 10^{21}\text{cm}^{-3}$ for PSD epi). These new process technologies provide a pathway to achieve the target ρ_c required for transistor performance in advanced logic devices.

INTRODUCTION

Contact resistance is one of the key challenges that needs to be addressed as FinFET scaling for 10-7nm node [1, 2]. Recent work [3] reported by Yu et al showed that NMOS ρ_c of $1.5 \times 10^{-9} \Omega\text{cm}^2$ with a Ge PAI and Astra™ DSA anneal on HDSi:P ($2 \times 10^{21}\text{cm}^{-3}$). Additionally, conformal doping using PLAD and dynamic surface anneal (DSA) with better fin sidewall doping coverage for HDSi:P epi, resulted in low NMOS ρ_c of $1.2 \times 10^{-9} \Omega\text{cm}^2$ [4]. For PMOS, an optimized implant sequence resulted in low ρ_c of $2 \times 10^{-9} \Omega\text{cm}^2$ on $\text{Si}_{0.3}\text{Ge}_{0.7}\text{:B}$ with Ti germanosilicidation [5]. Interestingly, in this reported study the first Ge PAI along with B implant followed by nanosecond laser anneal (NLA) enabled higher dopant incorporation and activation at the interface. Additional Ge PAI was performed before silicidation to form a high-quality silicide interface. Another recent study reported PMOS ρ_c of $1.9 \times 10^{-9} \Omega\text{cm}^2$ on group III element doped Ge with nanosecond laser annealing [6].

In this work, we report that optimizing the epi, implant and anneal techniques are paramount to reducing NMOS and PMOS ρ_c . We investigated the impact of Ge PAI with and without additional dopant implant, and compared different laser anneal techniques (millisecond laser anneal Astra™ DSA and NLA). Additionally, we report the effect of dopant species (Ga vs. B) in SiGe:B, and evaluated the effect of activation achieved by Astra™ DSA vs. NLA.

EXPERIMENT

Process flows used for NMOS & PMOS CC ρ_c test vehicles are summarized in Figs. 1 and 2, with key process steps described below: HDSi:P epi (for NMOS) and $\text{Si}_{0.55}\text{Ge}_{0.45}\text{:B}$ epi (for PMOS) were grown after STI/junction formation. After contact open, phosphorus or boron cryo (-100°C) implants for NMOS and PMOS were performed respectively, followed by laser anneal (DSA or NLA). Next, contact pre-clean (Siconi™), contact liner (PVD Ti/ ALD TiN) were applied, followed by silicide anneal at 600°C spike, CVD W fill, and W CMP. The low ρ_c enabling processes ($\text{Si}_{0.55}\text{Ge}_{0.45}\text{:B}$ epi, Ge, B and Ga implants, Siconi™, and NLA) were done using Applied Materials proprietary tools. Device-equivalent CC test vehicle (Fig. 3) with contact CD's ranging from 35-150nm was fabricated to evaluate ρ_c . By plotting CC resistance vs. diffusion length, ρ_c was extracted from the resistance values extrapolated to zero diffusion length, and

normalized with contact CD' (Fig. 3c). Detail of this method has been described in a previous publication [4].

RESULTS

Fig. 4 shows that optimal NLA conditions significantly reduce NMOS ρ_c to a record low $9.01 \times 10^{-10} \Omega\text{cm}^2$. Highly P-doped epi with optimized ion implant is required for NMOS ρ_c reduction, as shown in Fig. 5. Ge PAI is a key step to form smooth and high-quality silicide interface; up to 53% reduction in ρ_c was achieved with Ge PAI vs. no Ge PAI (Fig. 6) after NLA. Fig. 7 is a TEM image of CC with Ge PAI before laser anneal, revealing a thick amorphous layer created by Ge PAI. The TEM image in Fig. 8 shows that this amorphous layer crystallized after NLA.

Fig. 9 compares different laser anneal techniques, DSA and NLA for B activation in $\text{Si}_{0.55}\text{Ge}_{0.45}\text{:B}$ epi. It clearly shows that 67% improvement is achieved with NLA due to dopant super-activation and epi recrystallization. Fig. 10 shows PMOS ρ_c results for various ion implantation and NLA approaches. It is shown that ρ_c is reduced from 5.84×10^{-9} to $1.16 \times 10^{-9} \Omega\text{cm}^2$ by Ga I/I and NLA. Ion implantation into the contact provides high dopant concentration at interface and lowers the ρ_c . NLA enables super-activation of B in $\text{Si}_{0.55}\text{Ge}_{0.45}\text{:B}$ epi film [7]. PMOS ρ_c results with and without Ga/B implants vs. NLA energy fluence are shown in Fig 11. ρ_c decreases with increasing laser energy fluence and reaches a saturation level, indicating that at lower fluence, the amorphous layer begins to recrystallize, and it is fully converted to a crystalline layer at higher fluence. However, if the fluence is too high, it damages the contact hole and creates voids [7] that resulted in higher ρ_c . Fig. 12 shows STEM images of CC with either (a) low energy fluence or (b) high energy fluence. Higher fluence could melt the $\text{Si}_{0.55}\text{Ge}_{0.45}\text{:B}$ epi film as shown in Fig. 12(b). Comparison of EELS results in Fig. 13 and Fig. 14 shows that NLA can cause Ge atoms to diffuse to Si/SiGe epi interface. The effective dopant activation in the $\text{Si}_{0.55}\text{Ge}_{0.45}\text{:B}$ epi and contact interface is the dominant factors to reduce ρ_c .

CONCLUSIONS

We have successfully demonstrated advanced contact process techniques that provide pathways for NMOS and PMOS ρ_c improvement by integration of highly-doped epi films, cryo ion implantation and NLA super-activation. Optimization of implant and NLA conditions is critical for maximizing dopant activation, reducing defects and improving epitaxial regrowth, which resulted in low ρ_c . Ultra-low ρ_c values ($9.01 \times 10^{-10} \Omega\text{cm}^2$ for NMOS and $1.16 \times 10^{-9} \Omega\text{cm}^2$ for PMOS) on CC were achieved in this work. The super-activated dopants by implantation and NLA offer promising pathway to enable N and PMOS ρ_c to below $1 \times 10^{-9} \Omega\text{cm}^2$.

REFERENCES

- [1] B. B. DORIS, SHORT COURSE OF IEDM, 2015.
- [2] S.C. SONG ET AL., SYMPOSIUM ON VLSI CIRCUITS (VLSI CIRCUITS) 2015.
- [3] H. YU ET AL., IEEE IEDM 2015, P.592.
- [4] C.-N NI ET AL., SYMPOSIUM ON VLSI TECHNOLOGY 2016.
- [5] H. YU ET AL., SYMPOSIUM ON VLSI TECHNOLOGY 2016.
- [6] O. GLUSCHENKOV ET AL., IEEE IEDM, 2016.
- [7] CHIH-YANG CHANG ET AL., IWJT, 2017.

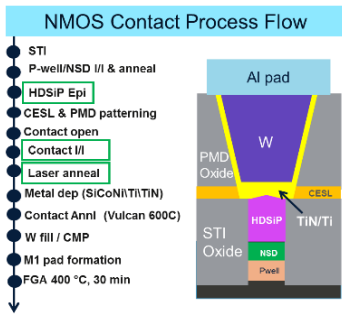


Figure 1. NMOS contact chain process flow on HDSiP Epi with P I/I splits and laser anneal for [P] activation.

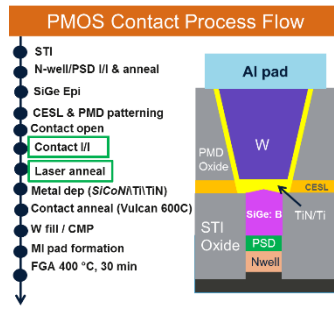


Figure 2. PMOS contact chain process flow on SiGe: B epi with B or Ga I/I and DSA or nsec laser anneal.

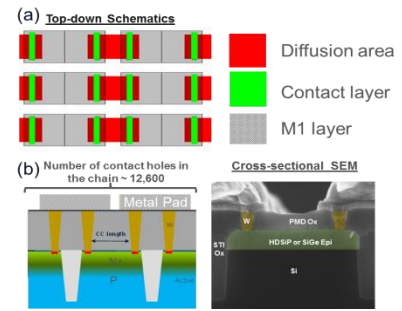


Figure 3. (a) Contact chain structures (top view); (b) (cross-section) of schematic and SEM image.

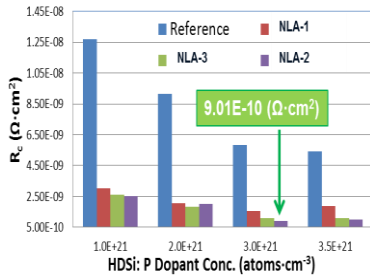


Figure 4. NMOS ρ_c as function of HDSiP dopant conc and NLA splits. All splits had Ge PAI. The P doping level varies from 1×10^{21} to 3.5×10^{21} atoms. cm^{-3} .

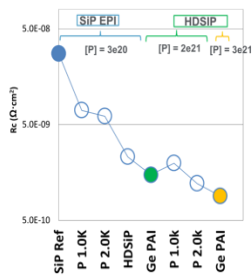


Figure 5. Pathway of NMOS ρ_c reduction with S/D epi doping level and ion implant.

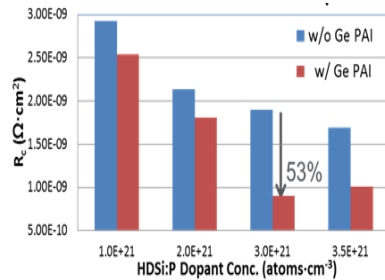


Figure 6. NMOS ρ_c reduction as function of HDSiP dopant conc w/ and w/o Ge PAI splits post NLA. Up to 53% ρ_c reduction was measured for HDSiP (3.0×10^{21} cm^{-3}) with Ge PAI and NLA.

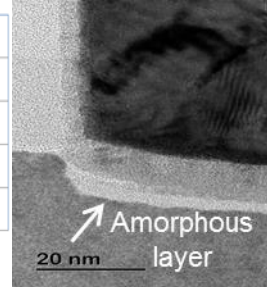


Figure 7. XTEM of contact hole without anneal. A thick amorphous layer is formed between HDSiP epi and Ti metal.

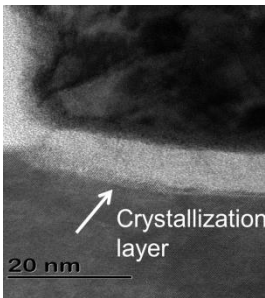


Figure 8. XTEM of contact hole with optimal NLA. NLA transforms the amorphous layer into crystalline layer, resulting in lower ρ_c .

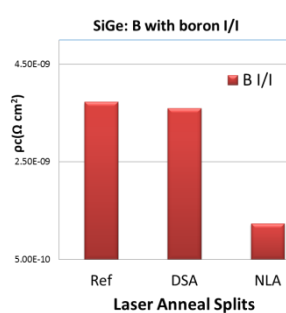


Figure 9. Comparison of DSA vs. NLA for B implanted SiGe: B.

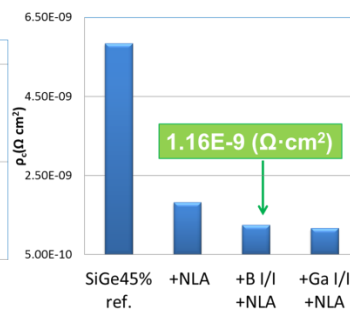


Figure 10. PMOS ρ_c vs. implant and anneal splits. ρ_c is reduced from 5.84×10^{-9} to 1.16×10^{-9} $\Omega \cdot \text{cm}^2$ by Ga I/I and NLA.

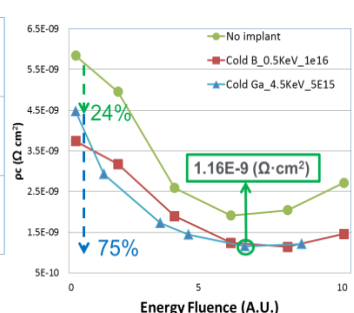


Figure 11. PMOS ρ_c for I/I splits vs. nsec laser energy fluence. Up to 75% ρ_c reduction is observed from 4.47×10^{-9} to 1.16×10^{-9} $\Omega \cdot \text{cm}^2$.

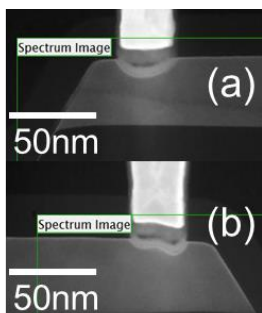


Figure 12. STEM images of PMOS contact chain with NLA (a) low and (b) high fluence.

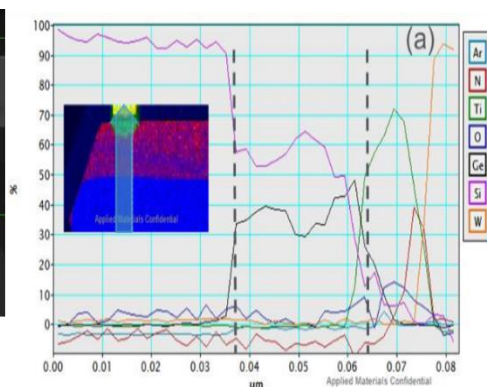


Figure 13. EELS results of low laser fluence indicate no Ge diffusion from epi film to Si.

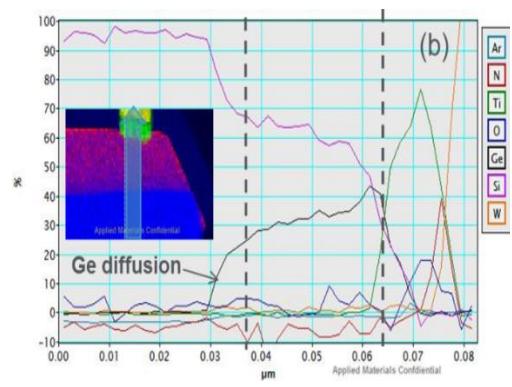


Figure 14. EELS results of high laser fluence indicate Ge diffusion from epi film to Si which damages the contact.